

**Molecular dynamics study of melting of the bcc metal vanadium. I. Mechanical melting**

V. Sorkin,\* E. Polturak, and Joan Adler

*Physics Department, Technion—Israel Institute of Technology, Haifa 32000, Israel*

(Received 8 May 2003; published 3 November 2003)

We present molecular dynamics simulations of the homogeneous (mechanical) melting transition of a bcc metal, vanadium. We study both the nominally perfect crystal and one that includes point defects. According to the Born criterion, a solid cannot be expanded above a critical volume, at which a “rigidity catastrophe” occurs. This catastrophe is caused by the vanishing of the elastic shear modulus. We found that this critical volume is independent of the route by which it is reached, whether by heating the crystal or by adding interstitials at a constant temperature which expand the lattice. Overall, these results are similar to what was found previously for an fcc metal, copper. The simulations establish a phase diagram of the mechanical melting temperature as a function of the concentration of interstitials. Our results show that the Born model of melting applies to bcc metals in both the nominally perfect state and the case where point defects are present.

DOI: 10.1103/PhysRevB.68.174102

PACS number(s): 64.70.Dv, 81.10.Fq, 61.72.Ji, 72.10.Fk

**I. INTRODUCTION**

Over the years, several theories explaining the mechanism of melting have been proposed.<sup>1–3</sup> This research has by now evolved to a state where a clear distinction exists between two possible scenarios for the melting transition: a first scenario of *homogeneous* or *mechanical melting* resulting from lattice instability<sup>4–6</sup> and/or a spontaneous generation of thermal defects<sup>7–11</sup> and a second scenario of *heterogeneous* or *thermodynamic melting* which begins at extrinsic defects such as a free surface or an internal interface (grain boundaries, voids, etc.).<sup>12–16</sup> Throughout this paper we will use the term “mechanical melting” to describe the former case, which we consider here. In particular, we take the view proposed by Born that at the melting point a *rigidity catastrophe* is caused by the vanishing of one of the elastic shear moduli<sup>4,5</sup>  $C_{44}$  or  $C' = (C_{11} - C_{12})/2$ . In other words, the crystal melts once it loses its ability to resist shear. This condition determines the mechanical melting temperature  $T_s$  of a perfectly homogeneous bulk crystal and was confirmed in extensive studies of fcc metals.<sup>10,11,17–19</sup>

Tallon<sup>5</sup> pointed out that a mechanical instability arises when the solid expands up to a *critical specific volume* which is close to that of the liquid phase (melt). In the study by Wang *et al.*<sup>17,18</sup> of the mechanical melting transition of an fcc solid under external stress, it was found that volume expansion is the underlying cause of lattice instability. Kanigel *et al.*<sup>11</sup> confirmed this scenario in a simulation of fcc copper in the presence of point defects. They showed that the critical volume at which a crystal of copper melts is independent of the path through phase space by which it is reached, whether by heating of the perfect crystal or by adding point defects to expand the solid at a constant temperature.<sup>11</sup>

Solids can undergo mechanical melting only if they have no extended defects,<sup>6</sup> a situation which is conveniently realized in three-dimensional computer simulations by means of periodic boundary conditions which eliminate the surface. Simulations of atomic dynamics for solids with an fcc<sup>10,11,17–19</sup> or diamond<sup>20</sup> structures show, among other things, the onset of a shear instability of the solid at a temperature  $T_s$ , which can exceed the thermodynamic melting

temperature  $T_m$  by some 20%, depending on the details of the potential.

Given the considerable degree of understanding of the melting process of fcc crystals, it is of substantial interest to see if the scenario of mechanical melting also applies to solids having a different lattice structure. We therefore decided to study mechanical melting of a bcc metal, vanadium, by means of computer simulations. We present details of the calculations in Sec. II. In Sec. III we describe the results of the simulation of some physical properties of vanadium with and without point defects. In Sec. IV we present molecular dynamics simulation results for mechanical melting in the presence of point defects. Finally, in Sec. IV, we discuss the implication of our results for the question of the microscopic mechanism of melting.

**II. SIMULATION DETAILS**

We model the bulk melting transition of vanadium using the molecular dynamics simulation<sup>21</sup> technique. The choice of vanadium has no special significance as we are only interested in the generic features of metallic solids with a bcc lattice symmetry. While various many-body potentials for fcc metals<sup>22–24</sup> have been developed and thoroughly tested in numerous simulations, the situation with such potentials for bcc metals is not as good. This can be explained by the more complicated nature of the bcc metals in comparison with fcc ones which manifests itself in the wide range of elastic constants. The packing density of atoms in a bcc lattice is smaller than in a fcc lattice (there are 8 nearest neighbors in a bcc lattice and 12 nearest neighbors in a fcc). However, the second nearest-neighbor distance in the bcc structure is larger than the first nearest-neighbor distance by only about 15%. Therefore, the interaction between the second-order and first-order nearest neighbors in bcc metals is not negligible, even with screening.

In addition, band structure effects are crucial for bcc metals. A simple approximation which assumes that the electron density can be considered as a superposition of atomic orbitals is successful for fcc metals, but less appropriate for bcc metals. Therefore, for metals with the bcc structure, the elec-

tron density is chosen to be an adjustable function, rather than a superposition of atomic orbitals. Furthermore, angle-dependent interactions could be very important in bcc solids.

For our simulations, we chose the many-body interaction potential developed by Finnis and Sinclair<sup>25</sup> (FS) and modified by Rebonato *et al.*<sup>26</sup> FS proposed a way to incorporate the delocalized physical nature of the metallic bonding and the essential band character of bcc metals in a simple model. The FS potential involves two short-ranged potentials:  $V = V_1 + V_2$ . The first potential  $V_1$  corresponds to an ion-ion interaction:

$$V_1 = \frac{1}{2} \sum_{i: i \neq j}^N \Phi(r_{ij}), \quad (1)$$

where  $\Phi(r)$  is the two-body part (ion-ion repulsion) and  $N$  is the number of atoms. The second potential  $V_2$  incorporates the complex nature of metallic cohesion:

$$V_2 = \sum_{i=1}^N U(n_i). \quad (2)$$

The function  $U(n_i)$  is taken to mimic the results of the tight-binding theory.<sup>25</sup> It depends on the electronic charge density  $n_i$  around the atom  $i$ :

$$n_i = \sum_{j: i \neq j}^{N_g} \rho(r_{ij}), \quad (3)$$

where  $N_g$  is the number of nearest neighbors of the atom  $i$  and the function  $\rho(r_{ij})$  is given by

$$\rho(r_{ij}) = \begin{cases} (r_{ij} - d)^2, & r_{ij} \leq d, \\ 0, & r_{ij} > d, \end{cases} \quad (4)$$

where  $r_{ji}$  is the distance between the atoms  $i$  and  $j$ , and  $d$  is a fitting parameter. Explicitly, the many-body part  $U(n_i)$  is given by

$$U(n_i) = -A \sqrt{n_i}, \quad (5)$$

where  $A$  is a fitting parameter.

Our molecular dynamics (MD) simulations with the FS potential were performed using the Parinello-Rahman<sup>27</sup> method, which allows simulation of fluctuations in the shape and volume of the sample. The Nose-Hoover thermostat was used to set the temperature.<sup>28,29</sup>

The equilibrium average shape and volume of the sample obtained at a given temperature were used for calculation of the shear modulus in a canonical ( $N$ - $V$ - $T$ ) ensemble<sup>30,31</sup>—i.e. at the fixed number of atoms,  $N$ , volume  $V$ , and temperature  $T$ .

The samples used for the simulations contained 2000 atoms, initially arranged as a perfect bcc crystal of size  $10 \times 10 \times 20$  unit cells. Periodic boundary conditions were applied in all three directions. Point defects were introduced either by the insertion of extra atoms between the lattice sites (self-interstitials) or by the removal of atoms from the lattice (vacancies). Newton's equations of motion were solved us-

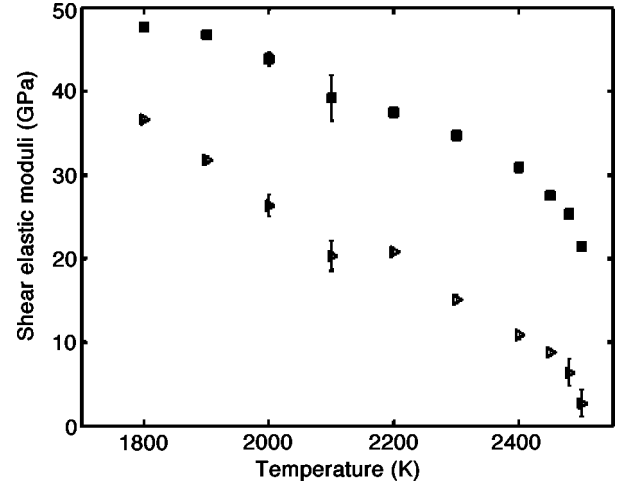


FIG. 1. Variation of  $C'$  (triangles) and  $C_{44}$  (squares) with temperature. The error bars represent the statistical uncertainty.

ing a predictor-corrector algorithm.<sup>21,32</sup> Throughout this study, interactive visualization with the AVIZ program<sup>33</sup> was implemented.

### III. VALIDATION OF THE POTENTIAL AND ORDER PARAMETER

To learn about the capability of the potential, we examined some physical properties of a perfect crystal. First, we calculated the thermal expansion at zero external pressure. We found the thermal expansion coefficient at low temperatures to be  $\alpha_c = (18 \pm 6) \times 10^{-6} \text{ K}^{-1}$ , in reasonable agreement with the experimental value measured at room temperature,  $\alpha_{\text{expt}} = 8.6 \times 10^{-6} \text{ K}^{-1}$ . Next, the thermodynamic melting temperature for our potential was calculated, using the method of Lutshko *et al.*,<sup>34</sup> to be  $T_m = 2220 \pm 10 \text{ K}$ . This value is close to the experimental value  $T_m = 2183 \text{ K}$ , despite the fact that the FS potential was constructed by fitting its parameters to room-temperature values of various physical properties of vanadium (lattice constant, cohesion energy, shear elastic moduli, vacancy formation energy, etc.).

In order to test the algorithm we calculated the shear moduli as a function of temperature. The shear elastic coefficients decrease with temperature as shown in Fig. 1. The accuracy of the simulations was estimated by monitoring the convergence of the shear elastic moduli calculated along symmetrically equivalent directions. We found the difference to be approximately 10%.

Following the validation that our potential can indeed reproduce the physical properties of a perfect crystal with acceptable accuracy, point defects were introduced. These point defects are distributed homogeneously throughout the bulk of the solid. Only one type of point defects—e.g., vacancies or self-interstitials—were used in each run to avoid their mutual annihilation.

The configurations of atoms in the vicinity of a point defect inside the bulk at low temperatures were investigated by means of the simulated tempering method.<sup>35,36</sup> The most energetically favored configuration of an interstitial was found to be the  $\langle 011 \rangle$  *dumbbell split interstitial* with a formation

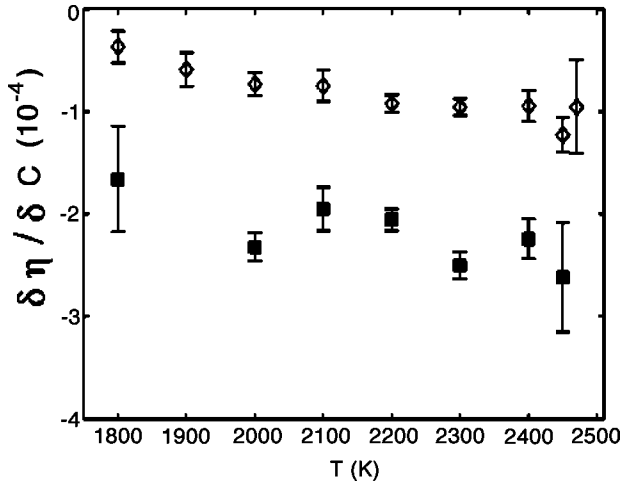


FIG. 2. Influence of point defects: vacancies (diamonds) and self-interstitials (squares) on the structure order parameter  $\eta$  as a function of temperature. The concentration of point defects,  $C$ , is given as a percent of the total number of atoms. The error bars represent the statistical uncertainty.

energy of  $E_f = 4.18 \pm 0.02$  eV. This formation energy is in agreement with that of previous simulations.<sup>37</sup>

To investigate the temperature dependence of the crystal-line order, we define the structure order parameter  $\eta$ :

$$\eta = \left\langle \frac{1}{N^2} \left| \sum_{i=1}^N \cos(\vec{k}\vec{r}_i) \right|^2 + \frac{1}{N^2} \left| \sum_{i=1}^N \sin(\vec{k}\vec{r}_i) \right|^2 \right\rangle, \quad (6)$$

where  $\vec{k} = \{0, 0, 2\pi/a\}$  is a vector of the reciprocal lattice,  $\vec{r}_i$  is the position of atom  $i$ ,  $N$  is the number of the atoms in the sample, and the angular brackets stand for ensemble average. For an ideal-crystal lattice at zero temperature,  $\eta$  equals unity, while in the liquid state,  $\eta$  fluctuates near zero.

We calculated  $\delta\eta/\delta C$ , the change of the order parameter upon the introduction of point defects. Here,  $C$  is the concentration of point defects, given in % of the number of atoms. Figure 2 shows the result of this calculation for small  $C$  ( $C \leq 1\%$ ) and at different temperatures. The introduction of self-interstitials results in a noticeable decrease of the structure order parameter (from  $\eta \sim 0.6$  to  $\eta \sim 0.4$ ), while the influence of vacancies is relatively weaker. With increasing temperature, the order parameter becomes increasingly sensitive to the introduction of point defects, as evidenced by the increase of the absolute value of  $|\delta\eta/\delta C|$  with temperature. We believe that this increased sensitivity results from the increase of the amplitude of the thermal vibration of the atoms in the immediate vicinity of the point defect.

The introduction of point defects results in a decrease of atomic density, as shown in Figs. 3 and 4. The specific volume of point defects at various temperatures was estimated using the linear dependence of the atomic density on the number of defects, apparent in Figs. 3 and 4. The volume of the sample at a small number of self-interstitials can be written as

$$V = Nv + N_{si}v_{si}, \quad (7)$$

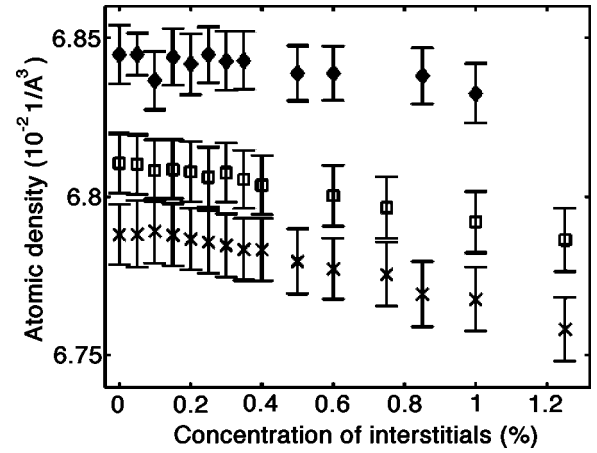


FIG. 3. Atomic density as a function of concentration of interstitials at several temperatures:  $T = 2300$  K (diamonds),  $T = 2200$  K (squares), and  $T = 2000$  K (crosses). The concentration of point defects is given as a percent of the total number of atoms. The error bars represent the statistical uncertainty.

where  $N$  is the number of atoms in the sample,  $v$  is the volume per atom in a perfect crystal of vanadium,  $N_{si}$  is the number of self-interstitials, and  $v_{si}$  is the volume per interstitial. Therefore the atomic density  $n$  is given by

$$n = \frac{N + N_{si}}{V} \approx \frac{1}{v} \left[ 1 - \left( \frac{v_{si}}{v} - 1 \right) \frac{N_{si}}{N} \right], \quad (8)$$

where the small concentration of point defects,  $N_{si}/N \ll 1$ , and approximate equality of the specific volumes,  $v_{si} \sim v$ , are taken into account.

A similar relation for the volume of vacancies can be written as

$$V = (N - N_{va})v + N_{va}v_{va}; \quad (9)$$

here,  $N_{va}$  is the number of vacancies and  $v_{va}$  is the volume per vacancy. The atomic density thus can be written as

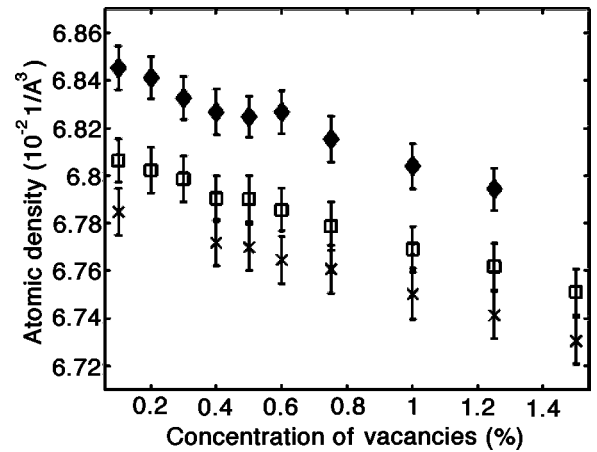


FIG. 4. Atomic density as a function of concentration of vacancies at several temperatures:  $T = 2300$  K (diamonds),  $T = 2200$  K (squares), and  $T = 2000$  K (crosses). The concentration of point defects is given as a percent of the total number of atoms. The error bars represent the statistical uncertainty.

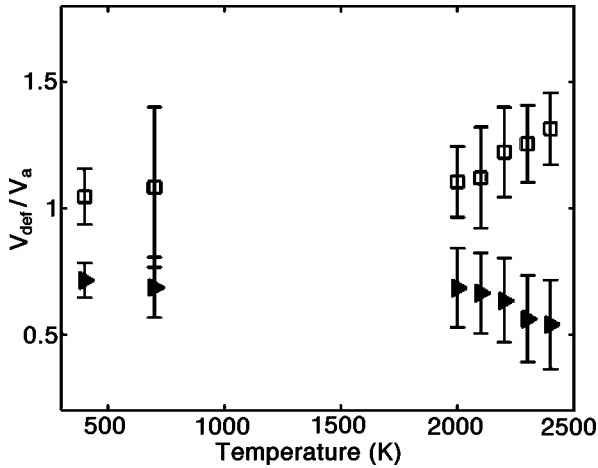


FIG. 5. The ratio of specific volume of point defects to the specific volume of an atom as a function of temperature: self-interstitials (squares) and vacancies (triangles). The error bars represent the statistical uncertainty.

$$n = \frac{N - N_{va}}{V} \approx \frac{1}{v} \left( 1 - \frac{N_{va} v_{va}}{Nv} \right). \quad (10)$$

It is interesting to point out that the linear dependence appears to hold even at temperatures close to  $T_s$ . This may indicate that the concept of a point defect remains meaningful even under these conditions. The specific volume of a point defect (in atomic volume units) is shown as a function of temperature in Fig. 5. It is seen that at temperatures above 2000 K these specific volumes change rapidly. To a large degree, this change can be accounted for by the rapid decrease of the elastic coefficients of the crystal in this temperature range.

#### IV. BULK MELTING TRANSITION

The prime goal of our simulations is the investigation of the role of point defects in mechanical melting. In the simulations of mechanical melting of fcc metals<sup>6,11,17</sup> it was found that the key parameter controlling melting is the volume of the crystal. It is well established that the mechanism of melting is a thermal elastic instability (the Born mechanism) which occurs when the shear elastic modulus vanishes. As we show below, the shear elastic modulus has a one-to-one correspondence with the molar volume. The latter is a more convenient parameter to describe the approach to melting in terms of critical volume, which does not depend on the path in phase space. When the Born criterion is applied to a superheated crystal lattice it establishes the existence of a critical volume above which the crystal becomes mechanically unstable and therefore undergoes a phase transformation to the liquid state or some other crystal structure. The critical volume is coupled with a maximum superheating temperature  $T_s$ . Simulations with fcc metals<sup>6,11,17</sup> showed that this critical volume  $v_s$  can be attained by expansion caused either by heating the crystal or by doping it with point defects at a constant temperature which expands the crystal,<sup>11</sup> or by pure mechanical dilatation at zero temperature.<sup>6,18</sup> In this sense

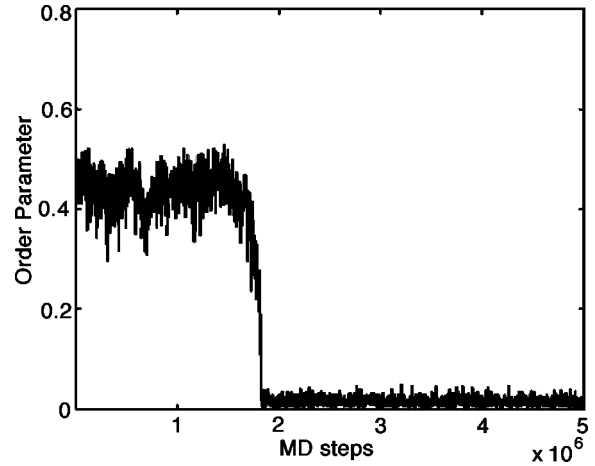


FIG. 6. Typical time dependence of the order parameter during mechanical melting. This particular sample contained 0.25% interstitials at temperature  $T=2475$  K.

the mechanical melting process appears to be universal; i.e., it is determined only by the sample expansion up to the critical volume.

In order to verify whether the same scenario holds in the case of a bcc metal we carried out simulations using samples with various concentrations of self-interstitials, or, alternatively, vacancies. The initial temperature of each sample was chosen far below the melting point of a perfect sample,  $T \approx 0.7T_s$ . As the samples were heated by gradually increasing the temperature, at some point we observed an abrupt decrease of the structure order parameter (see Fig. 6), together with a simultaneous increase of the total energy and volume (see Fig. 7). This event determines the mechanical melting temperature. The melting temperature of a sample without point defects is found to be  $T_s = 2500 \pm 20$  K. Since MD simulations are plagued by statistical fluctuations in the temperature and volume, in practice it is very difficult to reach the maximum superheating temperature  $T_s$ . Therefore, the accuracy in the determination of  $T_s$  in this way is about  $\sim 1\%$ .

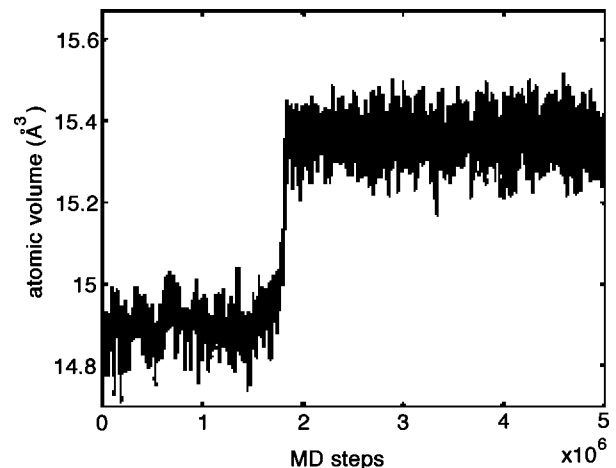


FIG. 7. Typical jump of the sample volume during the mechanical melting transition. This particular sample contained 0.25% interstitials at temperature  $T=2475$  K.

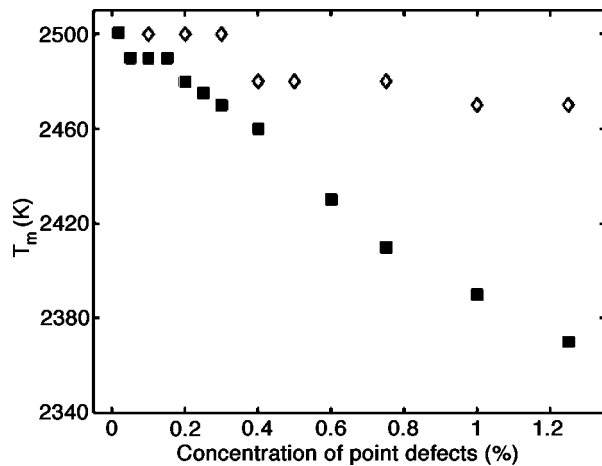


FIG. 8. The influence of interstitials (squares) and vacancies (diamonds) on the melting temperature of vanadium under periodic boundary conditions.

The same temperature  $T_s = 2500 \pm 12$  K was also found from a least-squares fit to the temperature dependence of  $C'$  as shown in Fig. 1. It is the temperature where  $C'$  goes to zero. This indicates that as is the case for fcc metals, homogeneous melting of the bcc metal results from a shear elastic instability. This particular value of  $T_s$  applies to a crystal of vanadium containing no defects and is about 280 K higher than the thermodynamic melting point  $T_m = 2220 \pm 15$  K obtained for our model using the method proposed by Luthsko *et al.*<sup>34</sup>

Once point defects are introduced, it is found that  $T_s$  becomes a function of their concentration. Results of simulations performed at different temperatures and defect concentrations are summarized in our phase diagram (see Fig. 8). The fact that point defects lower the melting temperature has been confirmed experimentally ( $\gamma$  irradiation lowers the melting point of pure metals by an amount proportional to the dose and thus to the number of generated point defects<sup>9,38</sup>). The lowering of  $T_s$  can be explained as follows: The introduction of self-interstitials leads to a significant local distortion of the bcc lattice and expands the volume of the solid (see Fig. 9). Therefore, a solid containing self-interstitials reaches its critical volume already at a lower temperature (the melting temperature is lower). In contrast, the effect of vacancies is rather minor, at least if their concentration is small enough. The same effect of lowering of the bulk melting temperature induced by interstitials was obtained by Kanigel *et al.*<sup>11</sup> for copper (fcc lattice). However, at higher concentrations of point defects the decrease of  $T_s$  cannot be explained simply by volume expansion. This is especially notable in the case of vacancies which have a smaller specific volume than the specific volume of an atom in a perfect crystal (see Fig. 5), but at high enough concentrations also lower the melting temperature (see Fig. 8). We refer here to the region in Fig. 8 where the concentration of point defects approaches 1%. These values are unrealistically large in comparison with the typical laboratory values of  $\approx 0.001\%$ . At these high concentrations, the concept of a single point defect is unclear and one should perhaps con-

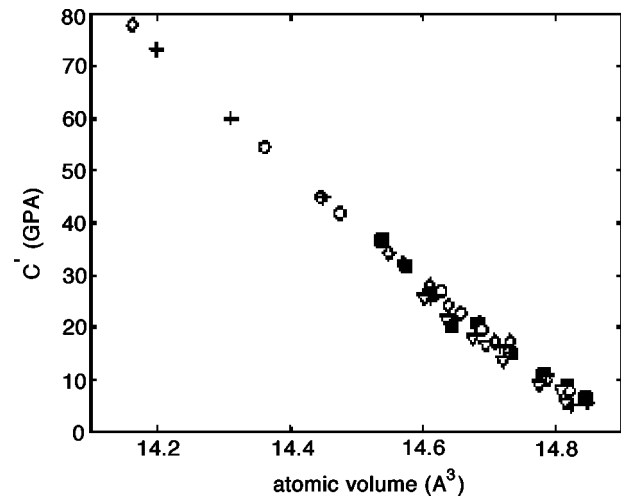


FIG. 9. Plot of the shear modulus  $C'$  against specific volume at various concentrations of interstitials: Squares: crystal without impurities (only thermal expansion). Diamonds: 0.05% concentration of interstitials. Circles: 0.1%. Triangles: 0.15%. crosses: 0.2%.

sider clusters or extended defects. According to Jin *et al.*<sup>19</sup> extended defects can act as nucleation centers for melting. Taking this point of view, the lowering of  $T_s$  with defect concentration may result from the combined effect of (a) volume expansion and (b) the introduction of nucleation centers for melting. Finally, it should be noted that the calculated phase diagram is qualitative, because of the finite sample size and limited simulation time.

Our results are broadly consistent with models of defect-induced melting proposed by Fecht<sup>39</sup> and Granato.<sup>7</sup> According to Fecht<sup>39</sup> melting is driven by the incorporation of point defects into the lattice. Point defects increase the probability of heterophase fluctuations of liquidlike clusters in the defective crystal and lower the Gibbs energy of the crystalline state. Therefore, the melting temperature decreases as the concentration of point defects increases.

The configuration of point defects (self-interstitials) in a fcc metals was exploited by Granato<sup>7</sup> to construct a model giving the thermodynamic properties of the crystalline and liquid states in a unified way. He found a large softening of the shear modulus with increasing defect concentration. This softening of the shear modulus caused by a change of lattice structure about point defects is called the diaelastic effect.<sup>7</sup> The restoring forces become weaker along certain directions in the presence of interstitials. This is reflected in the appearance of new low-frequency resonance modes and high-frequency local modes. The diaelastic softening of the shear modulus leads to a lowering of the formation energy for additional interstitials, which, together with the large entropy contribution from the new modes, lowers the melting temperature. In the above discussion, we have emphasized the role of lattice instability in establishing a maximum superheating temperature at zero external pressure. However, due to thermal expansion, any temperature change is accompanied by a simultaneous change of the volume. To decouple these two effects, we plot the dependence of the shear modulus  $C'$  on the specific volume in Fig. 9. As this figure shows, the dependence of  $C'$  on the specific volume appears to be

universal, in the sense that the value of  $C'$  is the same whether the volume at which it is calculated was reached at by thermal expansion or by insertion of point defects. In other words the main effect of interstitials is to expand the lattice. Using the data plotted in Fig. 9 one can extract the value of the critical volume  $v_s(T_s)$  at which the system melts homogeneously under the conditions of zero external stress.

Using this method we find  $v_s = 14.87 \pm 0.06 \text{ \AA}^3/\text{atom}$  and the melting temperature  $T_s$  for various concentrations of point defects. The critical volume is close to the specific volume of liquid vanadium at the thermodynamic melting temperature  $v_{liq} = 15.3 \pm 0.05 \text{ \AA}^3$  and to the experimental value<sup>40</sup> of  $v_{liq} = 15.2 \text{ \AA}^3$ .

Similar results were obtained for copper in MD simulations by Wang *et al.*<sup>17,18</sup> and by Kanigel *et al.*<sup>11</sup> It was found that the shear modulus vanishes at a lattice strain of  $a/a_0 = 1.024$ , where  $a$  is the lattice parameter at  $T_m = 1350 \text{ K}$  and  $a_0$  is the lattice parameter of copper at  $T_0 = 300 \text{ K}$ . The specific volume ratio of copper is  $(a/a_0)^3 = 1.07$  which is quite close to the value obtained for vanadium,  $v(T_m)/v(T_0) = 1.06 \pm 0.01$ . It is natural to ask whether the ratio  $a/a_0$  is universal, independent of lattice structure. To answer this question in a definitive manner, it would be useful to make similar simulations on other bcc metals.

## V. SUMMARY AND CONCLUSIONS

In our simulations we observed that each shear elastic modulus is a continuous and apparently universal function of the specific volume. The solid lattice can be expanded either by thermal expansion or by the presence of self-interstitials. The value of  $C'$  at any particular volume is independent of the way by which this volume was reached, either by thermal expansion alone or by any combination of thermal expansion and of expansion due to interstitials introduced into the sample at a constant temperature. The elastic energy of the lattice increases until a critical specific volume  $v_s$  (close to

the specific volume of the melt) is reached where the shear modulus  $C'$  vanishes, triggering mechanical melting. Upon melting, the solid transforms isothermally and discontinuously (see Figs. 6 and 7).

The process that triggers mechanical melting could be similar to the one observed by Jin *et al.*<sup>19</sup> in simulations of the melting of a surface-free Lennard-Jones crystal. There, melting occurs when the superheated crystal spontaneously generates a sufficiently large number of extended defects (clusters of spatially correlated destabilized particles which satisfy the Born criterion). Those extended defects play the role of surfaces in initiating the melting. In our simulations, point defects, especially in large concentrations where clusters of defects should be formed, could act as *nucleation centers* for these extended defects (molten regions) inside the solid.

This paper was devoted to a simulation of the melting process of a homogeneous bcc metal and its comparison with a similar process in fcc metals. It is of great interest to extend these simulations to heterogeneous melting which involves nucleation of the liquid phase at some preferred sites of the solid—for example, at the free surface. This study is the subject of a forthcoming paper.

## ACKNOWLEDGMENTS

We are grateful to Dr. G. Wagner, A. Kanigel, and Dr. J. Tal for their contributions to this project. The authors would like to acknowledge the use of computer resources belonging to the High Performance Computing Unit, a division of the Inter University Computing Center, which is a consortium formed by research universities in Israel. More information about this facility can be found at <http://www.hpcu.ac.il>. This study was supported in part by the Israel Science Foundation, the German Israel Foundation (GIF), and by the Technion VPR fund for promotion of research.

\*Electronic address: [phsorkin@techunix.technion.ac.il](mailto:phsorkin@techunix.technion.ac.il); URL: <http://phycomp.technion.ac.il/phsorkin/index.html>

<sup>1</sup>A. R. Ubbeldone, *Melting and Crystal Structure* (Clarendon, Oxford, 1965).

<sup>2</sup>F. Lindemann, *Z. Phys.* **11**, 609 (1910).

<sup>3</sup>Y. Ida, *Phys. Rev.* **187**, 951 (1969).

<sup>4</sup>M. Born, *J. Chem. Phys.* **7**, 591 (1939).

<sup>5</sup>J.L. Tallon, *Philos. Mag. A* **39**, 151 (1979).

<sup>6</sup>D. Wolf, P.R. Okamoto, S. Yip, J.F. Lutsko, and M. Kluge, *J. Mater. Res.* **5**, 286 (1990).

<sup>7</sup>A.V. Granato, *Phys. Rev. Lett.* **68**, 974 (1992).

<sup>8</sup>T.A. Weber and F.H. Stillinger, *J. Chem. Phys.* **81**, 5095 (1984).

<sup>9</sup>R.W. Cahn, *Nature (London)* **323**, 668 (1986).

<sup>10</sup>R.W. Cahn, *Nature (London)* **413**, 582 (2001).

<sup>11</sup>A. Kanigel, J. Adler, and E. Polturak, *Int. J. Mod. Phys. C* **12**, 727 (2001).

<sup>12</sup>J.W.M. Frenken and J.F. van der Veen, *Phys. Rev. Lett.* **54**, 134 (1985).

<sup>13</sup>J.F. van der Veen, in *Phase Transitions in Surface Films 2*, edited by H. Taub. *et al.* (Plenum, New York, 1991).

<sup>14</sup>A. Trayanov and E. Tossati, *Phys. Rev. B* **38**, 6961 (1988).

<sup>15</sup>R.N. Barnett and U. Landman, *Phys. Rev. B* **44**, 3226 (1991).

<sup>16</sup>E.T. Chen, R.N. Barnett, and U. Landman, *Phys. Rev. B* **41**, 439 (1990).

<sup>17</sup>J. Wang, J. Li, S. Yip, S. Phillpot, and D. Wolf, *Phys. Rev. B* **52**, 12 627 (1995).

<sup>18</sup>J. Wang, J. Li, S. Yip, S. Phillpot, and D. Wolf, *Physica A* **240**, 396 (1997).

<sup>19</sup>Z.H. Jin, P. Gumbsch, K. Lu, and E. Ma, *Phys. Rev. Lett.* **87**, 055703 (2001).

<sup>20</sup>S.R. Phillpot, S. Yip, and D. Wolf, *Comput. Phys.* **3**, 20 (1989).

<sup>21</sup>D. Rapaport, *The Art of MD Simulations* (Cambridge, University Press, Cambridge, England, 1991).

<sup>22</sup>S.M. Foiles, M. Baskes, and M. Daw, *Phys. Rev. B* **33**, 7983 (1986).

<sup>23</sup>K.W. Jacobsen, J.K. Norskov, and M.J. Puska, *Phys. Rev. B* **35**, 7423 (1987).

<sup>24</sup>F. Ercolessi and J.B. Adams, *Europhys. Lett.* **26**, 583 (1994).

<sup>25</sup>M. Finnis and J. Sinclair, *Philos. Mag. A* **56**, 11 (1987).

<sup>26</sup>R. Rebonato, D.O. Welch, R.D. Hatcher, and J.C. Billelo, *Philos. Mag. A* **55**, 655 (1987).

- <sup>27</sup>M. Parrinello and A. Rahman, Phys. Rev. Lett. **45**, 1196 (1980).
- <sup>28</sup>S. Nose, J. Chem. Phys. **81**, 511 (1984).
- <sup>29</sup>W. G. Hoover, Phys. Rev. A **31**, 1695 (1985).
- <sup>30</sup>J. Ray and A. Rahman, J. Chem. Phys. **82**, 4243 (1985).
- <sup>31</sup>J. Ray and A. Rahman, J. Chem. Phys. **80**, 4423 (1984).
- <sup>32</sup>M. P. Allen and D. J. Tildesley, *Computer Simulations of Liquids* (Clarendon, Oxford, 1987).
- <sup>33</sup>J. Adler, A. Hashibon, N. Schreiber, A. Sorkin, S. Sorkin, and G. Wagner, Comput. Phys. Commun. **12**, 623 (2002).
- <sup>34</sup>J.F. Lutsko, D. Wolf, S.R. Phillpot, and S. Yip, Phys. Rev. B **40**, 2841 (1989).
- <sup>35</sup>E. Marinary and R. Parisi, Europhys. Lett. **69**, 2292 (1992).
- <sup>36</sup>I. Yukito, Int. J. Mod. Phys. C **12**, 623 (2001).
- <sup>37</sup>G.J. Ackland and R. Thefford, Philos. Mag. A **50**, 313 (1987).
- <sup>38</sup>T. Goreski, Scr. Metall. **11**, 1051 (1977).
- <sup>39</sup>H.J. Fecht, Nature (London) **356**, 356 (1992).
- <sup>40</sup>*Handbook of Chemistry and Physics*, 81st ed., edited by D. R. Lide (CRC Press, Boca Raton, 2001).